Available online at www.sciencedirect.com
ScienceDirect
Chemical Physics Letters 431 (2006) 385–389
CHEMICAL PHYSICS LETTERS
www.elsevier.com/locate/cplett

Oxidative addition of methane and benzene C–H bonds to rhodium center: A DFT study

Siwei Bi *, Zhenwei Zhang, Shufen Zhu

College of Chemistry Science, Qufu Normal University, 21 Jingxuan West Road, Qufu, Shandong 273165, China

Received 2 July 2006; in final form 13 September 2006
Available online 23 September 2006

Abstract

A density functional theory study on mechanisms of the oxidative addition of methane and benzene C–H bonds to the rhodium center containing Cp and PMe_3 ligands has been performed. Our calculated results confirm that the C–H bond cleavage from a sigma complex to a hydride alkyl complex is the rate-determining step. Compared with the case of methane C–H bond, the oxidative addition of benzene C–H bond is more favorable kinetically and thermodynamically. Stronger backdonation from metal center to the σ^* antibonding orbital of benzene C–H bond is responsible for the observations.

1. Introduction

Alkanes and arenes can coordinate to transitional metal undergoing oxidative addition reaction (Scheme 1). The fact that a large number of transition metal complexes are able to activate arenes but not alkanes is surprising, on the basis of the observation that the bond energy of benzene C–H bond (around 110 kcal/mol) is larger than that of alkane C–H bond (around 95 kcal/mol) [1]. And, some reactions of arene C–H activation proceed faster than those of alkane C–H activation [2].

Using theoretical and computational methods to study the activation of unreactive carbon–hydrogen bonds has aroused great interests ever since the first presence of the intermolecular oxidative addition of alkane C–H bonds to transition-metal centers [3] .With great efforts to investigate the nature of the activation process in the past years [4,5], scientists explored the unsaturated transition-metal fragments of different structural types, employing methods such as semiempirical methods [6], various *ab initio* techniques [7] and density functional theory [8]. The calculation results have provided detailed and reasonable explanations for a large range of experimental results [9], which in turn demonstrates that quantum chemical calculations are reliable.

For example, $(C_5Me_5)Rh(PMe_3)H_2$ was irradiated in a mixed solvent system of propane/benzene at low temperature to afford $(C_5Me_5)Rh(PMe_3)(C_6H_5)H$ and $(C_5Me_5)Rh(PMe_3)(CH_2CH_2CH_3)H$. Experimental observations confirmed the reactions for benzene C–H activation were slightly faster than those for propane C–H activation. This paradox arouses our interest to explore the potential energy surfaces of such reactions using density functional theory (DFT). For the convenience of calculations, we used $(C_5H_5)Rh(PMe_3)H_2$ instead of $(C_5Me_5)Rh(PMe_3)H_2$, and methane instead of propane in the model reactions studied here (see Scheme 2).

2. Computational methods

Density functional theory (DFT) calculations at the B3LYP level [10] are carried out in order to explore the potential energy surfaces (PES) of the model reactions. The LANL2DZ effective core potential [11] is chosen for Rh and P, while the standard 6-31G(d, p) basis sets [12] are employed for the rest of atoms. Polarization functions [13] are added for phosphorus ($\zeta(d) = 0.34$). Experience has

* Corresponding author. Fax: +86 537 4456305.
E-mail address: siweibi@126.com (S. Bi).

0009-2614/$ - see front matter © 2006 Elsevier B.V. All rights reserved.
doi:10.1016/j.cplett.2006.09.049

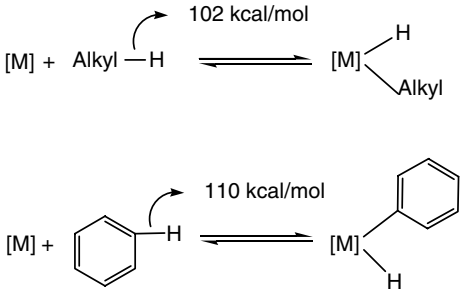

Scheme 1.

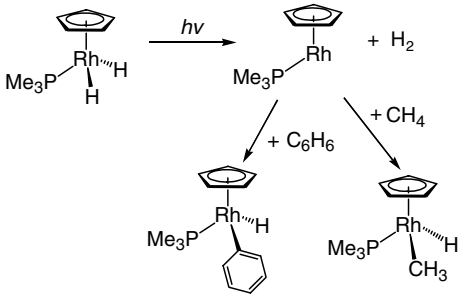

Scheme 2.

shown that this level of theory provides reasonable predictions for transition-metal-containing compounds [14]. Intrinsic reaction coordinate (IRC) [15] calculations allow us to interconnect the different structures located on the PES and then construct the energy profiles. All the calculations are performed with the GAUSSIAN 98 software package [16].

Considering the involvement of gas molecules (H_2, CH_4) in the reaction mechanisms, we used free energy to describe the potential energy profile. The enthalpic energy was given in bracket.

3. Results and discussion

3.1. Mechanism on the activation of H–CH_3

The energy profile on the reaction of CH_4 with $(C_5H_5)Rh(PMe_3)H_2$ is shown in Fig. 1. Three steps are involved in the reaction. The first step is the reductive elimination of H_2, the second one is the σ-bonding coordination of H–CH_3 to Rh center, and the final one is formation of a metal alkyl hydride complex through H–CH_3 oxidative addition.

The free energy change ΔG and the enthalpy change ΔH for the first step (**1**–**2**) are calculated to be 26.70 and 35.68 kcal/mol, respectively, indicating that this step is strongly unfavorable thermodynamically. Clearly, the conversion from an 18e species to a 16e species is responsible for the great thermodynamic data. As experiments confirmed, such kind of H_2 reductive elimination could be achieved through irradiation. The small ΔG compared with the ΔH is a result of entropy increase. Theoretical calcula-

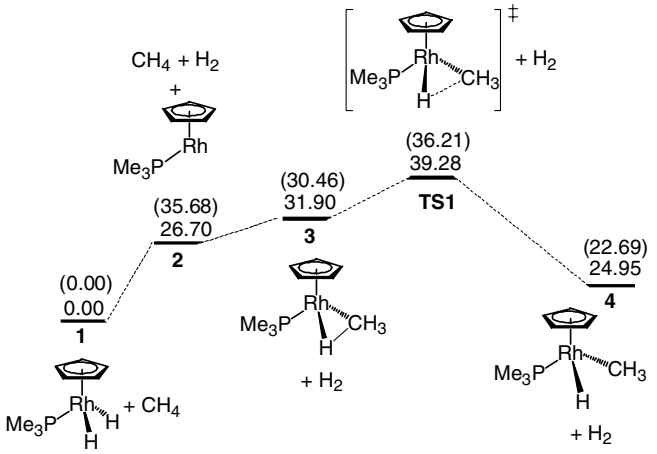

Fig. 1. Energy profile for the reaction of $CpRhH_2PMe_3$ with methane. Corresponding enthalpy was given in parentheses.

tions predict that the step is a non-barrier process and no non-classic Rh hydride intermediate is located. This may be resulted from the strong backdonation from Rh center to the antibonding orbital of H_2. The ability of backdonation of Rh is enhanced with the presence of the two strong electron-donating ligands, Cp and PMe_3. In the second step (**2**–**3**), one C–H bond of CH_4 is bonded to the metal center. The free energy change and the enthalpy change are calculated to be 5.20 and −5.22 kcal/mol, indicating that this step is unfavorable in free energy and favorable enthalpically. The free energy increase results from the entropy decrease from **2** to **3**, and the enthalpy decrease is due to the transformation from a 16e species to an 18e species. From **3** to **4**, the activation free energy and activation enthalpy are calculated to be 7.38 and 5.75 kcal/mol, respectively. The CH_3–H bond distance in **TS1** is 1.45 Å, larger than that in **3** (1.13 Å), and smaller than that in **4** (2.41 Å), meaning the CH_3–H bond is breaking. This step is thermodynamically favored with ΔG and ΔH being 6.95 and 7.77 kcal/mol, respectively. Product **4** is more stable than the intermediate **3**. This is because strong backdonation from Rh center to the antibonding orbital of CH_3–H strongly weakens the C–H bond and hence leads to the formation of strong Rh–H and Rh–CH_3 bonds. Also, product **4** is less stable than the reactant **1**. This is a result of the fact that the Rh–H bond is stronger than the Rh–Me bond. It can be seen from Fig. 1 that the CH_3–H bond cleavage is the rate-determining step.

Compared oxidative addition of H_2 (**2**–**1**) with that of CH_4 (**2**–**3**), it can be seen that the former reaction is a non-barrier process and no intermediate exists, while the latter reaction experiences an intermediate **3** and a transition state **TS1**. The reason for the phenomena is that 1s orbital of H atom is dense and nondirectional, favoring effective overlap with transition metal d orbitals and hence enhancing the interaction between Rh and H atom. The hybridized orbital of C atom is directional in space, which makes against effective overlap with transition metal d orbitals and hence weakens the interaction between Rh

and C atom, relative to the case of M–H. Thus, relatively stronger interaction of Rh with H_2 makes the molecular H_2 complex (intermediate) non-existent, while relatively weak interaction of Rh with CH_4 results in the existence of intermediate **3** (see Fig. 2).

3.2. Mechanism on the activation of $H–C_6H_5$

Fig. 3 shows the energy profile for the reaction of $CpRhH_2PMe_3$ with benzene. Fig. 4 illustrates the B3LYP optimized structures involved in the reaction. The first step (**1**–**2**) has been discussed above. The second step (**2**–**3**′) is the coordination of benzene to Rh center by using one pair of its π electrons, which has been confirmed to be a non-barrier process. In other words, no transition state is located. The free energy change and enthalpy change for the step are calculated to be 2.55, 15.68 kcal/mol, respectively, indicating this step is favorable both in free energy and in enthalpy. In contrast to the step (**2**–**3**), the free energy decreases as well. This is because the intermediate

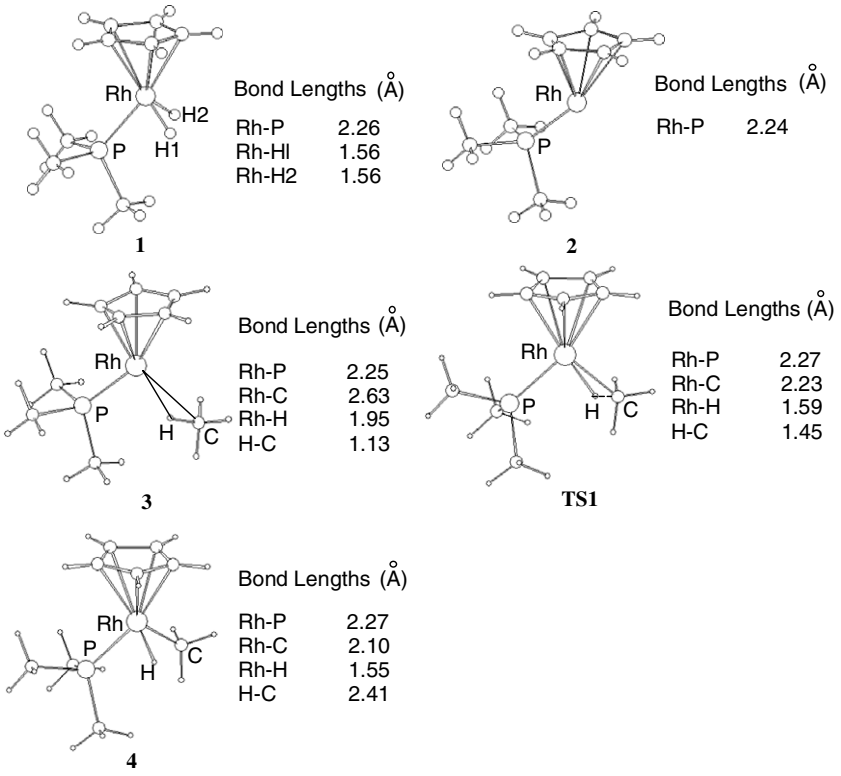

Fig. 2. Selected B3LYP optimized structures involved in the reaction of $CpRhH_2PMe_3$ with methane, together with selected bond distances. The bond distances are given in Å.

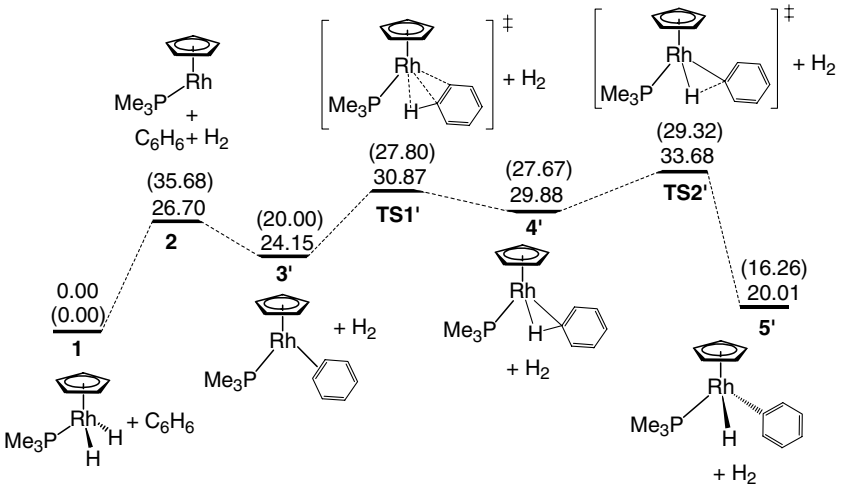

Fig. 3. Free energy profile for the reaction of $CpRhH_2PMe_3$ with benzene. Corresponding enthalpy was given in parentheses.

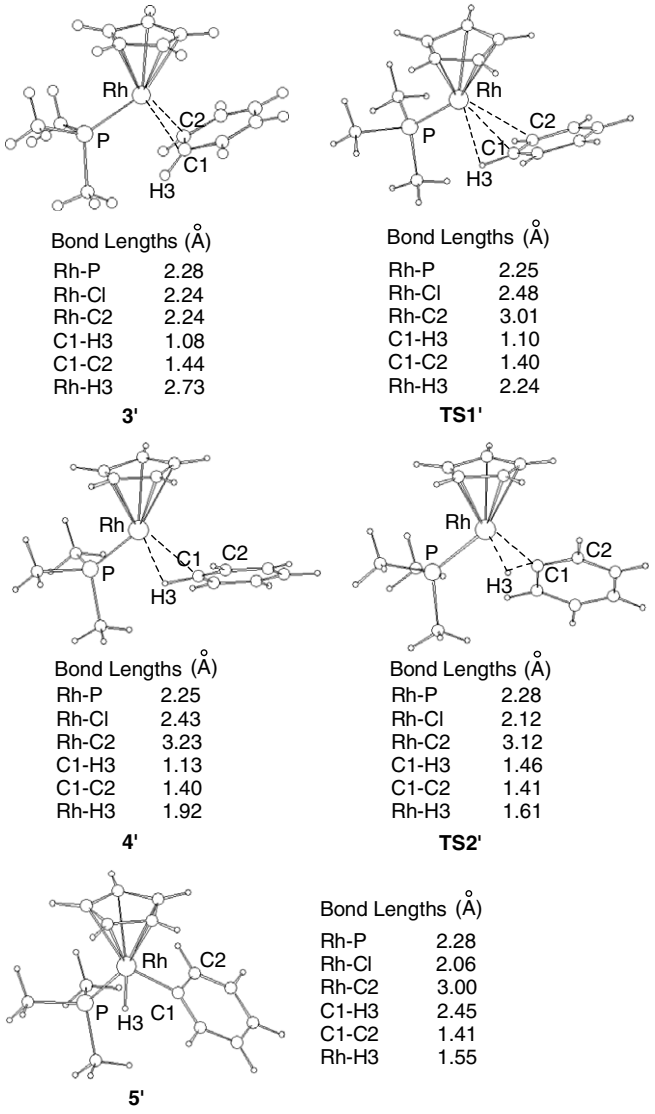

Fig. 4. B3LYP optimized structures involved in the reaction of $CpRhH_2PMe_3$ with benzene, together with selected bond distances. The bond distances are given in Å.

3′ is more stable than **3** as a result of the stronger backdonation from the Rh d orbital to the antibonding orbital of H–C_6H_5 bond. The third step is the bonding mode conversion. The C═C π electrons coordinate to the metal in **3′**, while the C–H σ bonding electrons coordinate to the metal in **4′**. A transition state, **TS1′**, is located. The activation free energy and activation enthalpy are calculated to be 6.72, 7.80 kcal/mol. Comparing the structural data of **3′** and **TS1′** (see Fig. 4), we can see that Rh–C1 and Rh–C2 bond distances increase, indicating that the π-electron bonding is weakened. The Rh–H3 bond distance becomes smaller (2.73–2.24 Å) and C1–H3 bond is elongated (1.08–1.10 Å), implying that the C1–H3 σ-bonding electrons are effectively coordinating to the metal center. In **4′**, C2 is far away from Rh atom, while C1 is slightly close to Rh. The C1–H3 bond distance becomes 1.13 Å, implying the bond is further activated. The σ-donation of C1–H3 to the metal and the backdonation from metal to the antibonding orbital of C1–H3 are responsible for the C1–H3 bond elongation. Correspondingly, the Rh–H3 distance becomes smaller (1.92 Å). Based on the data above, we can predict that the C1–H3 has bonded to the metal center. The free energy change and enthalpy change from **3′**–**4′** are calculated to be 5.73, 7.67 kcal/mol, respectively, indicating the step is thermodynamically unfavored. This is because the C–H bonding is weaker than the C═C bonding to the metal. The last step is the C–H bond breaking to form a Rh hydride phenyl product. The transition state, **TS2′**, is located. The activation free energy and activation enthalpy are calculated to be 3.8, 1.65 kcal/mol. Compared with **4′**, the C1–H3 bond in **TS2′** is further activated, supported by the bond length change from 1.13 Å in **4′** to 1.46 Å in **TS2′**. In the product **5′**, Rh–H and Rh–Ph σ bonds are formed. Our calculations show that the free energy change and enthalpy change from **3′** to **4′** are −9.87, −11.41 kcal/mol, indicating that this step is much more favored. Examining the overall energy profile shown in Fig. 3, we can see that the rate-determining step is still the C–H bond breaking.

3.3. Comparison between oxidative additions of CH_4 and C_6H_6 bond cleavage

As seen from Figs. 1 and 3 that the first step (**1**–**2**) is the same in both model reactions. The free energy change from **2** to **3** increases while that from **2** to **3′** decreases. This is because **3′** is more thermodynamically stable than **3** due to stronger backdonation from metal center to the antibonding π^* orbital of C═C double bond involved in **3′**, which overcomes the entropy decrease. **4′** and **3** have the same bonding mode where C–H bond is bonded to metal center by using its σ-bonding electrons, but **4′** is more stable than **3**. This is a result of the fact that the phenyl group is much more electron-withdrawing than the methyl group, making the level of the antibonding σ^* orbital of H–C_5H_6 to be lower than that of H–CH_3. Therefore, the backdonation from metal center to the C–H σ^* orbital is stronger in **4′** than in **3**. As has been mentioned above, the C–H bond cleavage is the rate-determining step for both reactions. The highest free energy for the reaction of H–CH_3 oxidative addition relative to **1** is 39.28 kcal/mol (**TS1**), while that for the reaction of H–C_6H_5 oxidative addition relative to **1** is 33.68 kcal/mol (**TS2′**), indicating that the former is less favored kinetically than the latter. One reason is that **4′** is more stable than **3**. What is more, the activation free energy (7.38 kcal/mol) for the cleavage of H–CH_3 bond (**3**–**4**) is greater than that (3.80 kcal/mol) for the cleavage of H–C_6H_5 bond (**4**–**5′**). The lower activation free energy from **4** to **5′** results from stronger backdonation from Rh center to the H–C_6H_5 σ^* antibonding orbital. The C–H bond distance (1.45 Å) in **TS1** is shorter than the C1–H3 bond distance (1.46 Å) in **TS2′** although the uncoordinated H–CH_3 bond is longer than the uncoordinated H–C_6H_5 bond, implying that the H–C_6H_5 bond is more strongly activated than the H–CH_3 bond. The small Rh–C bond dis-

tance (2.23 Å) in **TS1** compared with that (2.12 Å) in **TS2′** also indicates that stronger interaction between Rh and the C atom of benzene. This is understandable because the phenyl group is more electron-withdrawing than methyl group. **5′** (20.01 kcal/mol relative to **1**) is more thermodynamically stable than **4** (24.95 kcal/mol relative to **1**). Clearly, stronger Rh–C_6H_5 interaction compared with Rh–CH_3 interaction is responsible for the higher stability of **5′**.

4. Conclusions

Two reaction mechanisms on oxidative addition of H–CH_3 and H–C_6H_5 to the fragment $CpRhPMe_3$ were studied by using density functional theory. Reductive elimination of H_2 from $CpRhH_2PMe_3$ was calculated to be much kinetically and thermodynamically unfavorable. Experimentally, this step could be achieved with irradiation. For H–CH_3 oxidative addition a sigma Rh complex (**3**) is directly obtained, while for H–C_6H_5 oxidative addition a more stable η^2-arene Rh complex (**3′**) is first formed and then the corresponding sigma Rh complex (**4′**) is obtained *via* the transition state **TS1′**. Our results of calculations indicate that the rate-determining step is the C–H bond cleavage for both the reactions. The H–C_6H_5 oxidative addition is more favored than the H–CH_3 one both kinetically and thermodynamically, for which stronger electron-withdrawing of phenyl group compared with methyl group is responsible.

Acknowledgement

This work was supported by the National Science Foundation of China (No. 20473047).

References

[1] S.W. Benson, Thermochemical Kinetics, Wiley, New York, 1968, p. 309.
[2] W.D. Jones, F.J. Feher, Acc. Chem. Res. 22 (1989) 91.
[3] (a) A.H. Janowicz, R.G. Bergman, J. Am. Chem. Soc. 104 (1982) 352; (b) A.H. Janowicz, R.G. Bergman, J. Am. Chem. Soc. 105 (1983) 3929.
[4] (a) For reviews, see: G.W. Parshall, Acc. Chem. Res. 8 (1975) 113; (b) R.G. Bergman, Science 223 (1984) 902; (c) A.H. Janowicz, R.A. Perima, J.M. Buchanan, C.A. Kovac, J.M. Struker, M.J. Wax, R.G. Bergman, Pure. Appl. Chem. 56 (1984) 13; (d) C.L. Hill, Activation and Functionalization of Alkanes, Wiley, New York, 1989; (e) J. Halpern, Inorg. Chim. Acta 100 (1985) 41; (f) M. Ephritikhine, New. J. Chem. 10 (1986) 9; (g) W.D. Jones, F.J. Feher, Acc. Chem. Res. 22 (1989) 91; (h) A.D. Ryabov, Chem. Rev. 90 (1990) 403; (i) J.A. Davies, P.L. Watson, J.F. Liebman, A. Greenberg, Selective Hydrocarbon Activation, Principles and Progress, VCH Publishers, Inc., New York, 1990; (j) R.G. Bergman, J. Organomet. Chem. 400 (1990) 273; (k) N. Koga, K. Morokuma, Chem. Rev. 91 (1991) 823; (l) T. Ziegler, Chem. Rev. 91 (1991) 651; (m) R.G. Bergman, Adv. Chem. Series 230 (1992) 211; (n) E.P. Wasserman, C.B. Moore, R.G. Bergman, Science 255 (1992) 315; (o) R.H. Crabtree, Angew. Chem., Int. Ed. Engl. 32 (1993) 789; (p) D. Schroder, H. Schwarz, Angew. Chem., Int. Ed. Engl. 34 (1995) 1937; (q) A.J. Lees, A.A. Purwoko, Coord. Chem. Rev. 132 (1994) 155; (r) B.A. Amdtsen, R.G. Bergman, T.A. Mobley, T.H. Peterson, Acc. Chem. Res. 28 (1995) 154; (s) T. Ziegler, Can. J. Chem. 73 (1995) 743; (t) B.A. Arndtsen, R.G. Bergman, Science 270 (1995) 1970; (u) J.C. Lohrenz, H. Jacobsen, Angew. Chem., Int. Ed. Engl. 35 (1996) 130.
[5] (a) S. Niu, M.B. Hall, Chem. Rev. 100 (2000) 353; (b) P.E.M. Siegbahn, R.A. Blomberg, Chem. Rev. 100 (2000) 421.
[6] J.Y. Saillard, R. Hoffmann, J. Am. Chem. Soc. 106 (1984) 2006.
[7] A. Dedieu, Chem. Rev. 100 (2000) 543.
[8] (a) M. Torrent, M. Sola, G. Frenking, Chem. Rev. 100 (2000) 439; (b) G. Frenking, N. Frohlich, Chem. Rev. 100 (2000) 717.
[9] (a) G.H. Loew, D.L. Harris, Chem. Rev. 100 (2000) 407; (b) J. Alonso, Chem. Rev. 100 (2000) 637; (c) J.F. Harrison, Chem. Rev. 100 (2000) 679.
[10] C.S. Cramer, Essentials of Computational Chemistry. Theories and Models, Wiley, New York, 2002.
[11] (a) P.J. Hay, W.R. Wadt, J. Chem. Phys. 82 (1985) 270; (b) W.R. Wadt, P.J. Hay, J. Chem. Phys. 82 (1985) 284; (c) P.J. Hay, W.R. Wadt, J. Chem. Phys. 82 (1985) 299.
[12] W. Hehre, J.L. Radom, P.V.R. Schleyer, J.A. Pople, Ab initio Molecular Orbital Theory, Wiley, New York, 1986.
[13] S. Huzinaga, Gaussian Basis Sets for Molecular Calculations, Elsevier Science, Amsterdam, 1984.
[14] Chem. Rev. 100 (2000) 351–818. The whole issue is devoted to computational transition metal chemistry.
[15] (a) C. Gonza' lez, H.B. Schlegel, J. Chem. Phys. 90 (1989) 2154; (b) C. Gonza' lez, H.B. Schlegel, J. Chem. Phys. 94 (1990) 5523.
[16] M.J. Frisch et al., Gaussian 98, Revision A.9, Gaussian, Inc., Pittsburgh, PA, 1998.